

CHAPTER 6

EXPERIMENTAL PROCEDURE

Understanding the experimental approach is critical to understanding the validity and applicability of the experimental results presented in the other chapters. In this chapter, the experimental system and procedure used to acquire the data sets are discussed. First there is a brief overview of the entire experimental system. Then, the portion of the system responsible for forming the voltage pulse applied to the transducer is analyzed in detail due to the importance of linearity in the voltage source for our experiments. Lastly, the procedure utilized to obtain each data set will be explained.

6.1 Overview of Experimental System

A diagram illustrating the experimental setup is provided in Figure 6.1. The excitation system formed the backbone of the measurement system. It generated the high-voltage pulse that would be transmitted by the spherically focused ultrasound transducer (Matec/Valpey Fisher Instruments, Inc., Hopkinton, MA) as an acoustic wave. The acoustic pulse would then travel to the PVDF membrane hydrophone (Marconi, Ltd., Essex, England), which would translate it back into a voltage signal to be read by channel one on the digital oscilloscope (LeCroy Model 9354TM, Chestnut Ridge, NY). Channel 2 of the oscilloscope was used to monitor the voltage pulse applied to the transducer via a -40 dB signal sampler (SS-40, Ritec, Inc., Warwick, RI). The oscilloscope would then digitize the waveforms and perform the average over 100 pulses before sending the results to the computer (Dell Pentium-II). The computer saved the waveforms for later analysis and controlled the positioning system (Daedal Inc., Harrison City, PA) used to maneuver the hydrophone. The operation of some of these components of the system will be discussed in more detail in Section 6.3 as it relates to the acquisition of the individual measurements.

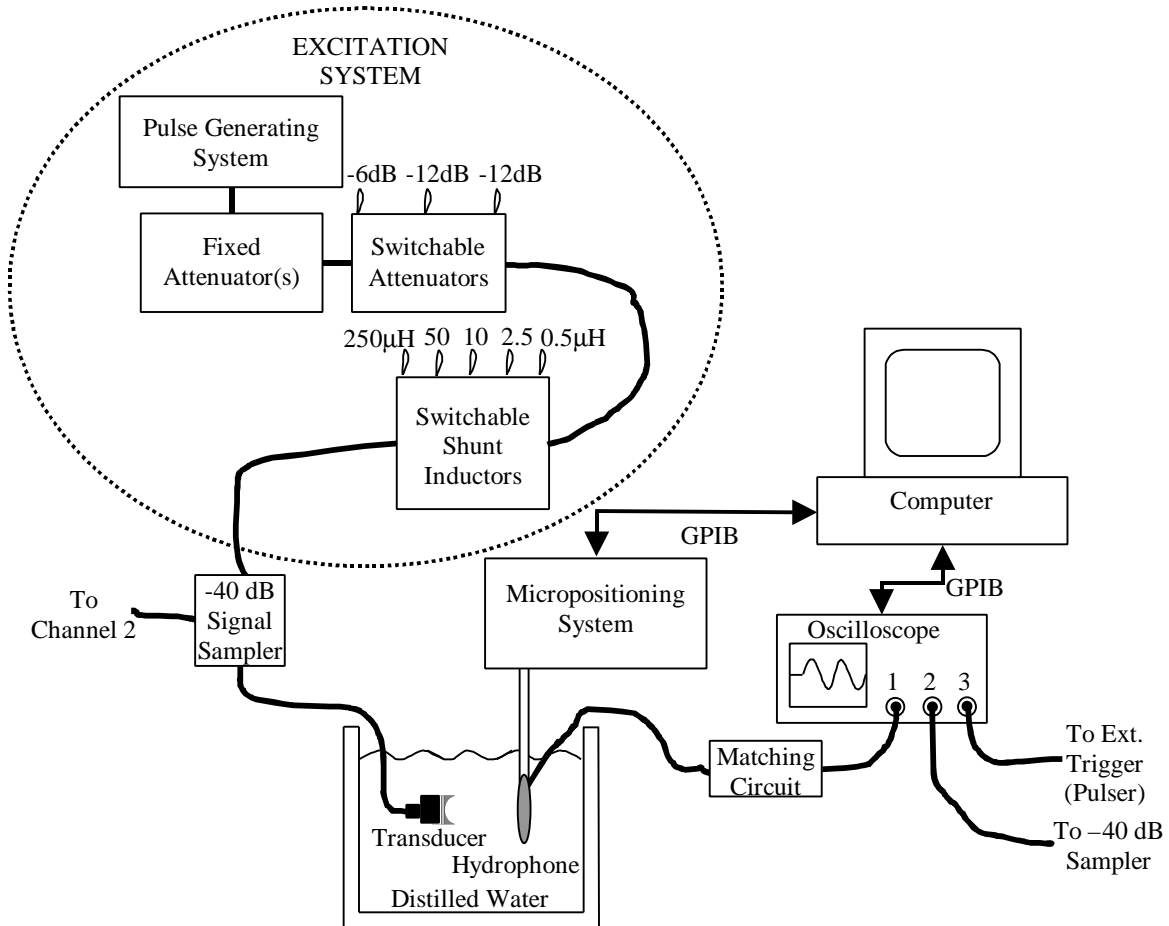


Figure 6.1: Diagram of experimental setup.

6.2 Analysis of Excitation System

Since the linearity of the excitation source is critical to any analysis of voltage-based linear extrapolation, special care needs to be taken in understanding the operation of the system used to excite the transducer. Referring back to Figure 6.1, the excitation system consisted of three parts: the pulse generating system, the attenuators, and the shunt inductors. Each of these will be analyzed in detail in this section of the thesis.

The pulse-generating system consisted of a computer controlling a high-power pulsed source (RAM5000, Ritec, Inc., Warwick, RI). The controllable parameters of interest for our measurements were the phase of the pulse, the pulse frequency, the number of cycles in the pulse, and the amplitude. The phase of the pulse refers to the phase of the sinusoid output by the pulse generator. Hence, a phase of 0° would generate a pulse that started at 0 V and then increased (i.e., positive going), whereas a phase of

180° would generate a pulse that started at 0 V and then decreased (i.e., negative going). The pulse amplitude was set by selecting an amplitude level in the range from 1 to 100 that the system translated into a voltage pulse. The relationship between the selected amplitude level and the resulting voltage was roughly linear.

The control parameters of pulse frequency and number of cycles refer to the selected primary frequency of the pulse and the selected number of complete cycles in the pulse. RITEC designed the pulse generator so that ideally the cycles would all be of equal amplitude emulating a sinusoid at the pulse frequency windowed by a perfect rectangular window. However, they also designed the source to drive a 50-Ω load. Therefore, when the pulse generator was connected to the reactive load of the transducer, the performance of the generator was degraded. Specifically, the number of cycles and frequency content of the pulse was severely affected. The procedures followed to restore the performance will be discussed shortly. For now, however, I want to emphasize that due to the transducer load, the number of cycles and the center frequency selected by the computer were not exactly the same as the number of cycles and the center frequency of the pulse applied across the transducer.

In order to illustrate the effect of the transducer load, the measured voltage pulse applied to the transducer was compared to the measured voltage pulse applied to a matched load under identical computer settings. The matched load was provided with the RAM5000 for the purpose of calibration. A plot illustrating the effect on one of the settings is provided in Figure 6.2. This particular measurement was made prior to the implementation of the procedures to restore the performance of the pulse generator. In this case, the central frequency set by the computer was 3.09 MHz and the number of cycles was set to one. The transducer used in this measurement had measured circuit resonant frequency of 2.9983 MHz, an $f/\#$ of 1, and a diameter of 5.08 cm.

Notice that the pulse shape and number of cycles have been severely distorted by the effects of the reactive transducer. Furthermore, there is a large dc component in the pulse. This dc component resulted from the increase in transducer impedance as the frequency decreased. Other measurements, which for sake of time will not be discussed, also indicated that when this lower frequency component was dominant, it would scale linearly as the amplitude setting of the computer was increased. However, the

frequencies actually transmitted by the transducer (i.e., frequencies around 3 MHz) would not scale in a linear fashion.

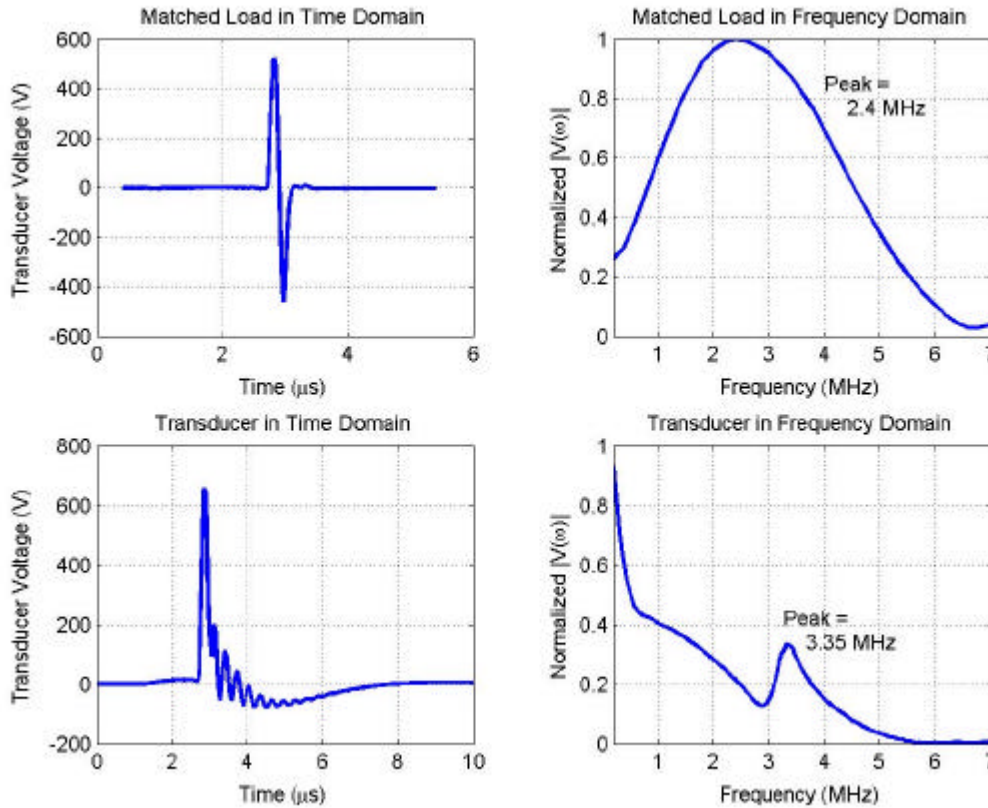


Figure 6.2: Pulses generated with matched load and transducer connected to the RAM5000.

Figure 6.2 also illustrates that although the pulse generated when the source is loaded by a matched load are closer to the settings selected by the computer, there is still some differences. The most notable difference is that the central frequency of the pulse is not the same as the frequency selected by the computer. Another effect that is more noticeable at higher frequencies is premature clipping of the pulse. The RAM5000 would tend to clip the last part of the last cycle. The clipping resulted from some timing problems in the circuitry of the pulse generator. Therefore, even in the ideal case, the settings supplied by the computer were not mirrored in the physical pulse generated. However, in this thesis, the voltage pulses applied to each transducer will still be referenced in terms of the central frequency, phase, and number of cycles selected by the computer. Hence, a “three cycle” “positive going” pulse (3p) at 2.9983 MHz would be a

pulse generated by setting the number of cycles to three, the frequency to 2.9983 MHz, and the phase to 0° in the computer menu.

Except for the excitation shown in Figure 6.2, the frequency selected by the computer was always set to the measured circuit resonant frequency reported in Table 5.2. The results shown in Figure 6.2 were obtained before the circuit resonant frequency was measured with the network analyzer as described in Chapter 5. As a result, the frequency selected corresponds to a previously measured peak in the radiated spectrum. However, the drive conditions under which this peak was obtained in the previous experiments are not known, so no comparison should be made between the two frequencies.

In order to improve the linearity of the applied voltage pulses and restore the pulse to its desired shape, attenuators and shunt inductors were included in the signal path. Two types of attenuators were included in the experimental setup, fixed attenuators (RA6, Ritec, Inc., Warwick, RI) and switchable attenuators (RA30, Ritec, Inc., Warwick, RI). Depending on the desired voltage range of transducer excitation, the number of fixed attenuators varied from one to two resulting in a change in the fixed attenuation from -6 dB to -12 dB. The switchable attenuators could also be switched into the circuit at any point in the measurement yielding a dynamic amount of attenuation from -30 dB to 0 dB in steps of 6 dB. The attenuators served three functions in the circuit. First, they isolated the transducer from the load so that the impedance of the load would not effect the operation of the pulse generator. A preliminary investigation indicated that approximately -6 dB of attenuation provided sufficient isolation and this number seemed to provide reasonable performance during the experiments as well.

Secondly, the attenuators allowed for simple linear scaling of the voltage pulse. Since the simplest linear element is a resistor, changing the value of a resistive network is the simplest method for inducing linear changes in a voltage. Therefore, in the experiment, the switchable attenuators could be switched into the circuit to improve the linearity of the source over a large dynamic range. However, the 6 dB step of the switchable attenuators was too large to allow the entire measurement to be performed by simply engaging the different attenuators. As a result, each data set was gathered by increasing the amplitude setting of the RAM5000 until the same peak to peak voltage

could be obtained at a lower amplitude setting with less attenuation. Then, the attenuation was reduced, and the amplitude settings were varied once again.

The third purpose of the attenuators that was particularly needful at the higher frequencies and $f/\#$'s considered in the experiment was to improve the overall dynamic range of the applied voltage pulse. Since the goal of the investigation was to determine when linear extrapolation would fail, the applied voltage pulse needed to vary in magnitude from well within the linear region to well into the nonlinear region. Furthermore, since some of the indicators of nonlinearity were no longer monotonic after a certain point, the voltage amplitude was increased as much as possible in order to capture this behavior. The switching attenuators could increase the dynamic range by a factor of 30 dB, and hence greatly increased the amount of information gathered in each data set.

As was previously mentioned, the second part of the restoration procedure was to include a strip of switchable shunt inductors (RSI-313, Ritec, Inc., Warwick, RI) prior to the transducer. The strip of inductors consisted of 5 inductors with values of 0.5 μH , 2.5 μH , 10 μH , 50 μH , and 250 μH , each of which could be placed in parallel with the signal path at any time by the flip of a switch. For our measurements, a value of inductance was selected and maintained for all the measurements on each transducer. The inductors acted as a loose matching network for the transducer. Recall from Chapter 5 and Appendix C that the transducer can be modeled as an RLC circuit whose dominant term, especially at low frequencies, is a parallel capacitance C_o . Therefore, the effect of the transducer can be reduced by including a parallel inductor that exactly cancels the impedance of the capacitor at resonance. Hence, the value of shunt inductance L_o , based on this matching scheme would ideally be given by

$$L_o = \frac{1}{(\omega'_o)^2 C_o} \quad (6.1)$$

Unfortunately, the strip of inductors could not yield the exact inductance specified by this formula for all of the transducers considered in the experiment. The ideal and implemented values of L_o for each of the transducers used in the experiment are provided in Table 6.1.

Table 6.1: Values used for the shunt inductance.

| Transducer $f/\#$ (Diameter) | Circuit Resonant Frequency | C_o | Ideal L_o | Implemented L_o |
|---------------------------------|-------------------------------|-----------|---------------|-------------------|
| 1 (1.905 cm) | 2.8072 MHz | 264.81 pF | 12.14 μ H | 10.00 μ H |
| 1 (5.08 cm) | 2.9983 MHz | 730.46 pF | 3.858 μ H | 2.500 μ H |
| 1 (1.905 cm) | 5.4906 MHz | 360.47 pF | 2.331 μ H | 2.359 μ H |
| 2 (1.905 cm) | 5.3574 MHz | 360.86 pF | 2.446 μ H | 2.500 μ H |
| 1 (1.905 cm) | 8.1517 MHz | 312.29 pF | 1.221 μ H | .5000 μ H |

Notice that in Table 6.1, for some of the transducers, the values of the shunt inductors used were much closer to the desired values given by Equation (6.1). Specifically, the 8.1517 MHz has the largest difference between the two values. Not surprisingly, the errors in the linear extrapolation for this transducer were also the largest as discussed in Chapter 5. Although some past measurements on the RAM5000 have indicated the performance deteriorates, specifically the clipping problem, for higher frequency pulses, poorer matching might also be a contributing factor to the increased error. This is promising for real ultrasound systems, since the transducer and drive circuitry for this case are typically very well matched hence the resulting voltage pulses should vary in a very linear fashion.

In order to conclude our discussion of the restoration procedure, a plot showing an example voltage pulse after the shunt inductance and attenuators have been included is shown in Figure 6.3.

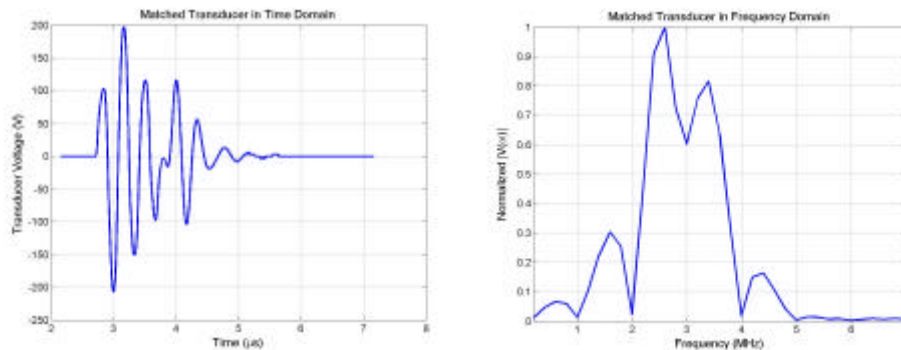


Figure 6.3 Voltage pulse after implementation of restoration procedures.

These results were also obtained by exciting the transducer with a circuit resonant frequency of 2.9983 MHz, a $f/\#$ of 1, and a diameter of 5.08 cm. However, this time, three cycles, instead of one cycle, were selected by the computer to reduce the effect of clipping in the RAM5000 generator, and the frequency selected to by computer was the measured circuit resonant frequency of the transducer. Notice that although the pulse is not perfect, the overall shape has been greatly improved. Furthermore, whereas before there was a strong dc component, now most of the energy is concentrated at the desired frequency band around 3 MHz.

At this point, we can generalize our discussion of the excitation system to other measurement systems. Recall that the setting of the pulse properties at one part in our circuit (i.e., on the computer menu) did not result in the same properties being present in our final pulse due to the effect of loading by the transducer. Based on these results, we can conclude that unless the transducer and the pulse generator are matched, one cannot determine the voltage pulse applied to the transducer by a measurement made prior to the final amplifier stage. Although for any system the voltage before the final stage can act as a reference, the reference value must be calibrated by real measurements before quantitative arguments can be made concerning the shape and amplitude of the waveform. Unfortunately, researchers are not always aware of this need [*Shen and Li, 2001*].

6.3 Data Acquisition

In this portion of the thesis, the procedure followed to acquire the data will be explained. As has been stated previously, different data sets were acquired for the different transducers and drive conditions in our experiment. Each data set consisted of a series of measurements that recorded the pressure waveform “close” to the transducer, the pressure waveform at the focus of the transducer, and the voltage pulse applied across the transducer. In the measurements, the voltage applied to the transducer was varied by changing the amplitude of the pulse selected by the computer in the pulse generator and by changing the appropriate attenuator settings. All the measurements for a given transducer and drive condition were obtained before any changes were made in either the

transducer or the drive conditions. In this experiment, “drive condition” refers to the number of cycles and phase set by the computer for a particular transducer.

The first step in any data set was to find the focus of the transducer. Before the focus can be found, the location of the focus needs to be defined. Normally for pulsed systems, the focus is defined as the location of the maximum pulse intensity integral (PII). However, this quantity cannot be directly observed on an oscilloscope. Therefore, we relaxed this definition and defined the focus to be the location of maximum peak-to-peak pressure. This location was found by moving the hydrophone along one of the axes of the scanning system until a maximum was found. Then the hydrophone was moved along another one of the axes until another maximum was found. The process was repeated sequentially for all three axes of the micropositioning system until there was a clear decrease in the peak to peak pressure as one moved away from a certain spatial location along any of the positioning axes. This location was then defined as the focus for the data set.

Furthermore, the step size required to observe a clear decrease was recorded as a possible error in the focus location. A table recording the required step sizes for each of the transducers is provided in Table 6.2. Notice that the larger $f/\#$ transducers typically required a larger step size since the area of the focal region was larger.

Table 6.2: Step sizes used to find the location of the focus for each transducer.

| Transducer $f/\#$ (Diameter) | Circuit Resonant Frequency | Wavelength | “Transverse” Step Size | “Axial” Step Size |
|---------------------------------|-------------------------------|----------------------|---------------------------|----------------------|
| 1 (1.905 cm) | 2.8072 MHz | 528.20 μm | 100 μm | 200 μm |
| 1 (5.08 cm) | 2.9983 MHz | 494.31 μm | 100 μm | 100 μm |
| 1 (1.905 cm) | 5.4906 MHz | 270.20 μm | 50 μm | 200 μm |
| 2 (1.905 cm) | 5.3574 MHz | 277.02 μm | 100 μm | 500 μm |
| 1 (1.905 cm) | 8.1517 MHz | 181.92 μm | 50 μm | 100 μm |

In Table 6.2, “Transverse” refers to the two positioning axes approximately transverse to the beam axis, and “Axial” refers to the axis approximately along the beam

axis. The wavelength provided is based on the central frequency set by the pulse generator and the sound speed. The sound speed was calculated based on the mean temperature for each data set. For the 5.4906 MHz transducer, the temperature used was the average of the three mean temperatures for the three data sets obtained for this transducer. All three of these data sets for this transducer were obtained on the same day based on the same focal and “close” location.

After finding the focus of the transducer, the next step was to set the location at which the “close” pressure waveforms would be recorded. This was done by moving the hydrophone as close as possible to the transducer along the axis of the positioning system that corresponded approximately to the beam axis of the transducer. The distances of the “close” location from the focus along this axis and movement information on how the position was changed during the measurement for each of the transducers studied is provided in Table 6.3.

Table 6.3: “Close” locations for each transducer.

| Transducer f/# (Diameter) | Circuit Resonant Frequency | Distance Along Axis | Movement Velocity | Movement Acceleration |
|------------------------------|-------------------------------|------------------------|----------------------|--------------------------|
| 1 (1.905 cm) | 2.8072 MHz | 10 mm | 1 mm/s | 0.1 mm/s ² |
| 1 (5.08 cm) | 2.9983 MHz | 28 mm | 2 mm/s | 0.1 mm/s ² |
| 1 (1.905 cm) | 5.4906 MHz | 8.7 mm | 2 mm/s | 0.1 mm/s ² |
| 2 (1.905 cm) | 5.3574 MHz | 32 mm | 2 mm/s | 0.1 mm/s ² |
| 1 (1.905 cm) | 8.1517 MHz | 9 mm | 1 mm/s | 0.1 mm/s ² |

Motion was limited by the fact that the plat on which the hydrophone was mounted was larger than the aperture of the transducer. As a result, the hydrophone was approximately located at the center of the aperture opposite the curved surface of the transducer as illustrated in Figure 6.4.

After setting the location of the “close” pressure waveform, the hydrophone was moved back to the focus, and the dynamic range of the excitation was confirmed. This was done by trying the maximum excitation setting and confirming that definite

asymmetric distortion was present in the waveform at the focus. Care was also taken to insure that the initial excitation was well within the linear approximation for propagation.

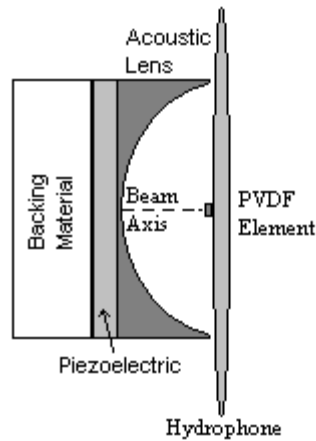


Figure 6.4: Diagram illustrating location of “close” pressure measurement.

At this point, we are ready to discuss the procedure followed to obtain the data at each excitation setting. First, the waveform at the focus and the voltage across the transducer was captured/averaged by the digital oscilloscope using a computer program provided with the LeCroy oscilloscope. Then the temperature of the water for the current excitation condition was recorded with a digital thermometer that reported the temperature to the tenth of a degree Celsius. The temperature did not vary significantly over the course of acquiring the data set for any of the experiments; however, it was still monitored to insure stability in our measurement. Another quantity that was monitored and recorded was the peak-to-peak voltage of the excitation pulse as read off of the digital oscilloscope. This was done to insure that the excitation voltage was increasing in the expected manner. This voltage could also be used as a quick reference at the time of data analysis.

After the temperature and voltage were recorded, the hydrophone was moved to the “close” location, and this pressure waveform was captured/averaged by the computer. The hydrophone was then moved back to the focus, the excitation voltage was increased, and the measurement was repeated. However, the location of the waveform was monitored during each measurement to confirm that the positioning system was consistently returning the hydrophone to the same location. Notice that all three

waveforms were recorded and stored by the oscilloscope/computer at the same time. No changes were made in the excitation system between measurements, and the RAM5000 pulse generator was left on until all of the waveforms had been saved to the computer.